PHYSICAL REVIEW B VOLUME 19, NUMBER 12 15 JUNE 1979

Stochastic theory of multistate diffusion in perfect and defective systems. II. Case studies

Uzi Landman and Michael F. Shlesinger
School of Physics, Georgia Institute of Technology, Atlanta, Georgia 30332
(Received 9 November 1978)

The time development of a number of physical systems can be described in terms of the temporal passage of the system through its allowable states. These states may correspond to spatial configurations, energy levels, competing transition mechanisms, or correlated processes. The evolution of certain of these systems can be analyzed by mapping onto a continuous-time random walk on a lattice whose unit cell may contain several internal states. In addition, we study the influence of periodically placed defects, which modify transition rates, on transport properties in several condensed-matter systems. A propagator formalism is reviewed where the matrix propagator (whose dimensions equal the number of internal states in a unit cell) is renormalized owing to the presence of defects. Knowledge of the propagator allows the evaluation of observable quantities such as positional moments, diffusion coefficients, occupation probabilities of states, and line shapes of scattering from diffusing particles. The formalism allows the study of diverse transport systems in a unified manner. We study the multistate diffusion of particles and clusters (specifically dimers) observed via field-ion microscopy on defective surfaces and derive expressions for observables pertinent to the analysis of these experiments. The lattice structure dependence of particle diffusion in systems containing defects which influence their neighbors is demonstrated. Next, the anomalous, non-Arrhenius behavior of the vacancy diffusion constant, observed via tracer-diffusion measurements, is described in terms of competing monovacancy mechanisms: nearest-neighbor and next-nearest-neighbor single jumps, and double jumps in which two atoms jump almost simultaneously, collinearly, as suggested by recent molecular-dynamics studies. We derive an analytic expression for the vacancy diffusion which provides a reinterpretation of fits to experimental data. As a further application of our method we investigate non-Markovian transport due to relaxation effects. Finally, we provide an analytic expression for the scattering law, $S(\vec{k},\omega)$, of quasielastic neutron scattering and demonstrate the non-Lorentzian line shape of the scattered intensity for systems containing defects and for correlated motion.

I. INTRODUCTION: TRANSPORT AND INTERNAL STATES AND DEFECTS

Studies of transport phenomena in condensed-matter systems provide information about the physical parameters of the underlying mechanisms governing the motion.[1] These parameters (activation energies, transition-frequency factors, structural factors, and correlation functions) reflect both potential and structural characteristics of the system under study. The degree of microscopic detail concerning the nature and the mechanism of transport depends upon the experimental resolution and range of data available and upon the method of analysis. The above is intimately connected with such characteristic spatial and temporal parameters of the system as correlation lengths and relaxation times.

In order to achieve a level of description compatible with the experimental resolution it is often convenient (and in fact sometimes necessary) to decompose the transport process into kinetic elementary steps. Often the stochastic evolution of the system via transition between these steps can be mapped onto a random-walk lattice with multiple states in each unit cell (which we call the internal states[2,3]). The number and type of internal states reflect the degree of microscopic knowledge of the process.

The mapping of kinetic steps onto a multiple-internal-state random-walk lattice serves as a unifying element in the analysis of a diverse variety of transport and reaction phenomena. For example, atomic and molecular clusters adsorbed on crystalline surfaces are observed, by means of field-ion microscopy (FIM), to exist in several geometric configurations.[4] The cluster-centroid motion traverses a random-walk lattice with several internal states per unit cell representing the allowed configurations. As discussed previously,[2,5,6] a proper analysis of FIM diffusion data (positional moments and configuration occupation probabilities) allows a determination of the individual transition rates between configurations, thus yielding a spectroscopy of the internal states of the cluster. Analysis which disregards the existence of the above internal states (i.e., analysis based upon the conventional semilogarithmic plot of the cluster-centroid positional variance $\sigma^2(t)$ versus $1/k_BT$) is inadequate for the determination of the pertinent diffusion parameters.

The mapping onto a multiple-internal-state random-walk lattice is not restricted to actual

distinct physical spatial configurations, but may represent states of the system in a generalized sense. For example, in an early study of surface diffusion by Lennard-Jones[7] a model has been introduced based upon two states of the migrating particle: one state in which the particle vibrates about the equilibrium position and another in which the particle migrates (the mobile state). This model can be mapped onto a random-walk lattice with two states in each unit cell (see Fig. 5, which in addition to the two internal states includes a defect site). As a further application of our general procedure, in Sec. IV we investigate diffusion via monovacancy mechanisms. We show that the deviation from the Arrhenius behavior of the diffusion constant at temperatures close to the melting point of the material,[8-11] can be explained[12] by including several *competing monovacancy mechanisms* which are activated at these elevated temperatures. Again, the solution to this problem is achieved via a mapping onto a multistate random-walk lattice. As a final example we consider (in Sec. V) a mode of transport in which correlation between steps exists in the sense that the departure of a particle (or a propagating excitation) from a site depends (in a time-dependent fashion) upon its last jump [i.e, for a one-dimensional system the particle would leave a site with (different) probabilities which depend upon whether it arrived there from the left or right]. The random-walk lattice for the correlated motion is obtained by mapping the above events onto a lattice (see Fig. 9). In Sec. VI we evaluate the quasielastic neutron scattering line shape from diffusing species whose motion is correlated.

Most crystalline systems contain imperfection to various degrees, due to a variety of sources. Defects occur either as an intrinsic property of crystals (such as thermally activated point defects, interstitials, and vacancies, which are present in the equilibrium structure of crystals at above-zero temperatures[13]), or may be voluntarily or involuntarily (contamination) introduced.

Defects and impurities are known to alter particle transport in crystalline systems.[14] In addition, they influence rates of surface-catalyzed reactions[15] and enter the theory of heterogeneous, active site-catalyzed, processes.[16] Thus it is of importance to understand the physical mechanisms involved in the above systems and to formulate theoretical methods through which the characteristics of the defects and transport processes can be determined via the analysis of experimental data (FIM, tracer diffusion, quasielastic neutron scattering, Mössbauer line shapes, and excitation diffusion in molecular systems).

In the previous paper[17] (which will hereafter be referred to as Paper I), we have developed the mathematical formalism of continuous-time random walks in multistate systems which contain a periodic arrangement of defects.[18] Defects are characterized by modified transition rates from the allowable states compared to the ideal (defect-free) host-lattice case. The change is expressed in the distribution function governing transitions, which reflects the potential characteristics of the system. We show that the particle propagator is "renormalized" owing to the presence of defects. Knowledge of the propagator allows the derivation of expressions for a number of observable quantities [moments of particle or vacancy position, equilibrium occupation probabilities of sites, and quasielastic neutron scattering line shapes (Sec. VI)], in a unified fashion.

The analysis presented in this study is for systems in which the defects form a (periodic) superlattice. Examples of physical systems in which such structures occur are transport in ordered alloy and multicomponent systems, ordered overlayer assemblies,[19] and ordered overlayer adsorption-surface systems.[20] For systems in which defects occur randomly, the coherent-potential-approximation (CPA) method may be applied.[21,22]

The paper is organized in the following manner: A brief summary of pertinent expressions derived in Paper I is given in Sec. II. In Sec. III we discuss several case studies of multistate diffusion on defective lattices and calculate the effect of defects and their concentration on the diffusion constants and probabilities of occupation of sites. We also show, in Sec. III B, that for systems in which defects influence transition characteristics of their nearest-neighbor sites, the diffusion constant depends upon the lattice structure. In Sec. IV we propose and analyze competing monovacancy diffusion mechanisms as the origin of the observed deviations from Arrhenius behavior of the diffusion constant as a function of temperature. Time-dependent correlated motion is studied in Sec. V. In Sec. VI we derive a general formula for the scattering law of neutrons scattered quasielastically from diffusing species. We apply the general formula to obtain non-Lorentzian line shapes for single-particle diffusion in a three-dimensional (3D) defective crystal and for a time-dependent correlated migration of a particle in 1D.

II. SYNOPSIS OF MATHEMATICAL FORMALISM

The mathematical formalism of random walks on periodic lattices with multiple internal states has been described elsewhere.[2,3,5] In Ref. 2 (Sec. V) and Paper I we have discussed diffusion

on lattices containing a periodic arrangement of defects, treated as internal states. A different method for treating propagation on periodic defective lattices, one which facilitates the calculations of basic transport quantities (in particular for small defect concentrations), via a renormalized propagator, has also been discussed by us in detail in Paper I. In this section we briefly review the pertinent elements of the theory of multistate transport on ideal and defective periodic lattices.

The basic quantity of the theory, which characterizes the temporal and spatial (structural) dependence of transitions performed by the propagating species is the waiting-time density function

$$\Psi_{ij}(\vec{l},\vec{l}';\tau)\equiv p_{ij}(\vec{l},\vec{l}')\psi_{(\vec{l}',j)}(\tau), \tag{2.1}$$

where $\vec{l}$ denotes a lattice-site location and j represents an internal state. $\Psi_{(\vec{l}',j)}(\tau)d\tau$ is the probability that a transition will occur from $(\vec{l}',j)$ in the time interval $(\tau,\tau+d\tau)$, given that the particle obtained $(\vec{l}',j)$ at $\tau=0$. This function is not an explicit function of $(\vec{l}',j)$, but is written in terms of parameters which characterize the state $(\vec{l}',j)$. These parameters reflect the potential characteristics of the state $(\vec{l}',j)$. In our studies we have chosen the following form for the waiting-time probability density function:

$$\psi_j^{(0)}(\tau)=\lambda_j^{(0)}e^{-\lambda_j^{(0)}\tau},\quad \psi_{(\vec{l}',j)}(\tau)=\lambda_j e^{-\lambda_j t}, \tag{2.2}$$

where $\lambda_j^{(0)}$, λ_j are the total transition rates for leaving internal state j, associated with ideal and defective sites, respectively; $p_{ij}(\vec{l},\vec{l}')$ is the probability that, given the occurance of a transition from state $(\vec{l}',j)$, it will lead to the occupation of state $(\vec{l},i)$. In general, $p_{ij}(\vec{l},\vec{l}')$ may also depend on the time τ at which the transition occurs (such an example is discussed in Sec. V).

The semi-Markovian evolution of the transport system can be studied in terms of the probability propagator $R_{ij}(\vec{l},t\,|\vec{l}_0,0)$, which is the probability density of reaching $(\vec{l},i)$ *exactly* at time t, having started at $(\vec{l}_0,j)$ at $t=0$, independent of the number of steps taken.

On an ideal lattice, with m internal states per lattice site, we have found in matrix notation that

$$\underline{R}^{(0)}(\vec{k},u\,|\vec{l}_0,0)=[\underline{1}-\underline{p}^{(0)}(\vec{k})\underline{\psi}^{(0)}(u)]^{-1}e^{i\vec{k}\cdot\vec{l}_0}, \tag{2.3}$$

where the superscript (0) indicates that these quantities are for a perfect lattice, the matrices are of dimension $m\times m$, and the propagator has been Fourier transformed over space $(\vec{l}\to\vec{k})$ and Laplace transformed over time $(\tau\to u)$ [see Eq. (2.3) and Appendix A in Paper I].

For a lattice with a periodic arrangement of defects, forming a defect superlattice of unit cell size $(\alpha l_x,\beta l_y,\gamma l_z)$, where l_x, l_y, and l_z are the host-lattice unit-cell length and α, β, and γ are integers, we have derived in Paper I the equation for the probability propagator $\underline{R}$ [see Eqs. (2.23) and (2.27) of Paper I] valid for all $\vec{k}$ and u values. While the complete expression for $\underline{R}$ is rather complicated, it may be observed that for calculations of physical quantities in the long-time (diffusion) limit a reduced form of the propagator can be used. The probability propagator in its reduced form is given as [see Eq. (2.28) in Paper I],

$$\underline{R}(\vec{k},u;z)=\{[\underline{R}^{(0)}(\vec{K},u;z)]^{-1}-\Omega\,\underline{D}(K,u)e^{-i\vec{k}\cdot\vec{l}_0}\}^{-1}, \tag{2.4}$$

where the components of $\vec{K}$ are

$$0\le K_x<2\pi/\alpha,\quad 0\le K_y<2\pi/\beta,\quad 0\le K_z<2\pi/\gamma,$$
$$\Omega=(\alpha\beta\gamma l_x l_y l_z)^{-1},$$

and the defect matrix $\underline{D}$ is given by

$$\underline{D}(\vec{K},u;z)=z\sum_{\{d\}}[\underline{p}_{(\vec{l},i)}(\vec{K})\underline{\psi}_{(\vec{l},i)}(u)-\underline{p}^{(0)}(\vec{K})\underline{\psi}^{(0)}(u)], \tag{2.5}$$

where the sum extends over all defects in *one* of the equivalent groups of defects which repeat periodically (denoted by $\{d\}$). Equation (2.4) for the probability propagator, in analogy to other usages of propagator techniques, can be interpreted as a renormalization of the ideal-lattice propagator $\underline{R}^{(0)}(\vec{k},u;z)$ by a "self-energy" correction due to the differences between defective and ideal lattice sites. The conditional probability P of being at state $(\vec{l},i)$ at time t [starting from $(\vec{l}_0,j)$ at $t=0$] is related to the propagator R via

$$P_{ij}(\vec{l},t\,|\vec{l}_0,0)=\int_0^t R_{ij}(\vec{l},t-\tau\,|l_0,0)\left(1-\int_0^\tau\psi_{(l,i)}(\tau')d\tau'\right)d\tau$$
$$\equiv\int_0^t R_{ij}(\vec{l},t-\tau\,|\vec{l}_0,0)\Phi_{(\vec{l},i)}(\tau)d\tau, \tag{2.6}$$

where the function $\Phi_{(\vec{l},i)}(\tau)$, defined above, accounts for the event that the system reached $(\vec{l},i)$ at an earlier time $t-\tau$ and remains there at time t.

Physical quantities of interest, such as spatial and temporal moments of the probability distribution and equilibrium occupation probabilities of states, can be derived from the above as discussed in detail in Paper I [Eqs. (2.33)–(2.42), and Sec. III and IV of Paper I]. In the following we investigate several physical transport systems using the above method, and discuss methods of analysis of experimental data.

III. CASE STUDIES OF MULTISTATE DIFFUSION

In this section we discuss several condensed-matter diffusion systems, and investigate the effects of defects and internal states on the diffusion mechanisms and implications of the above in the analysis of experimental observations.

A. Single-particle diffusion on a 1D defective lattice

The migration of particles and clusters on solid surfaces under controlled conditions can be observed on an atomic scale, by means of the ingenious methods of field-ion microscopy (FIM).[4] These measurements provide quantitative data about the diffusion process in terms of particle (or cluster-centroid) spatial moments [mean position (in case of a biased experiment[2,5]) and variance] and the equilibrium occupation of sites in the allowed configurations (in the case of a migrating cluster). From FIM data, one can determine such characteristic quantities of the diffusion mechanism as activation energies, frequency factors, diffusion constants, information concerning pairwise interaction potentials between adatoms, and cluster dissociation energies.[23] Consequently, FIM constitutes a microscopic spectroscopic tool for the investigation of solid surfaces.

Until now, most[24] FIM diffusion studies have been performed on perfect-crystal planes, and the one-dimensional and two-dimensional motions of particles and particle clusters of various sizes have been studied. We have previously suggested methods for the analysis of FIM data and have given a procedure by which transition rates of individual steps (between internal states) of the migration mechanism can be extracted from the experimental results.[2,5] In the following we investigate the motion of a single particle on defective periodic surfaces and suggest the possibility of obtaining, from FIM measurements on such surfaces, information about characteristic parameters of the defects.

We consider first a one-dimensional (1D) motion of a single particle [such as that observed in the channeled motion of a W atom on the (211) face of tungsten[25]]. As seen from Eq. (I2.53), the position variance for particle diffusion on a 1D lattice of spacing l and transition rate a for jumping to nearest-neighbor sites is given by $\sigma^2(t)=al^2t$. If $\sigma^2(t)$ is measured for known l for a sequence of times, the rate a can be found. When the experiment is performed at various temperatures and an activated Arrhenius form is used for a (i.e., $a=\nu_a e^{-E_a/k_BT}$, where E_a is the activation energy for a transition and T is the absolute temperature), E_a and the frequency factor can be determined from a plot of $\ln\sigma^2(t;T)$ vs $(k_BT)^{-1}$.

When defects are introduced substitutionally[24] into the lattice in a periodic manner at locations nl (where n is the period of the defect superlattice)

$$\sigma^2(t)=nl^2abt/[b(n-1)+a], \tag{3.1}$$

where b is the rate of leaving a defect. (Note that the effect of the defect has been assumed to be localized, although more general cases can be treated.) If the rate a is known from the perfect-lattice case, b can be found from the relation

$$a\sigma^2(t)/[anl^2t-(n-1)\sigma^2(t)]=\nu_b e^{-E_b/k_BT}=b. \tag{3.2}$$

Consequently, data obtained at different temperatures permit the determination of the defect parameters ν_b and E_b [from a plot of the logarithm of the left-hand side vs $(k_BT)^{-1}$]. Note that the usual practice of plotting $\log\sigma^2$ vs $(k_BT)^{-1}$ will not yield ν_a and E_a as the intercept and slope of a straight line, since only a and b, but not σ^2, are in an activated form.

When the rate a cannot be determined independently, a relation between the rates a and b, obtained via detailed balance for occupation of sites, [see Eqs. (I2.42a) and (I2.42b)] can be used:

$$P_{\rm eq}(\text{defect})=\Omega\lim_{u\to 0}uR_d(k=0,u)\Phi_d(u), \tag{3.3}$$

where, in our case, $\Omega=1/n$. The above yields

$$P_{\rm eq}(\text{defect})=\frac{1}{nb}\lim_{u\to 0}u\left[1-\frac{a}{a+u}-\frac{1}{n}\times\left(\frac{b}{b+u}-\frac{a}{a+u}\right)\right]^{-1}$$

$$=\frac{a/n}{a/n+b(1-1/n)}. \tag{3.4}$$

Thus, if the equilibrium population of the defect sites is recorded, the above relation supplements the equation obtained from the measurement of the variance in position, and a and b can be determined from these two relationships.

B. Single-particle diffusion on defective 2D lattices of different structures

We examine now the diffusion of single particles on two-dimensional square, hexagonal, face-centered-square and -triangular lattices in the presence of defects. We show that when a defect influences the transition rates of its neighbors, a structure (topology) dependence of the diffusion rate emerges. If the defect does not influence its neighbors, the diffusion rate on the different lattices is the same as long as the transition rates for leaving normal and defective sites are common

to them, and the jump lengths and defect concentrations are the same.

To motivate our analysis we consider first random walks of a single particle on perfect lattices of different structure (with the same bond length and the same rate of leaving sites). Obviously, under these circumstances the probability for the mean number of steps n taken in time t is the same for these lattices. The mean-square distance traveled after n steps is

$$\langle R_n^2\rangle = \left\langle \sum_{i=1}^{n}\sum_{j=1}^{n} \vec{r}_i \cdot \vec{r}_j \right\rangle , \tag{3.5}$$

where the average is over all possible paths, with equal probability of jumps along connecting bonds, and $\vec{r}_i$ is the displacement caused by the ith step. Since the jumps are uncorrelated,

$$\langle R_n^2\rangle = \left\langle \sum_{i=1}^{n} r_i^2 \right\rangle = n\langle r_i\rangle^2 = nL^2 \tag{3.6}$$

independent of the lattice connectivity (structure).[1]

If equivalent localized defects in equal concentrations are placed periodically in equal concentrations on these different lattices, then the diffusion constant for particles on these lattices will remain independent of lattice structure. This is due to the fact that the probability of occupying a defect site as $t\to\infty$ (the diffusion limit) is independent of the lattice structure for the cases described above, as can be seen from Eq. (3.3). Thus, in the limit of $t\to\infty$, the same number of jumps occur on each lattice, with the defect- and normal-site equilibrium occupation probabilities being the same for each lattice. When the defects effect their nearest neighbors, so the effective defect concentrations are no longer equal, a structural effect will appear, as shown in the following examples.

a. Rectangular lattice. Consider a defective rectangular lattice (Fig. 1) in which a migrating particle leaves a defect site with rate D, the four nearest neighbors to the defect site with rate B,

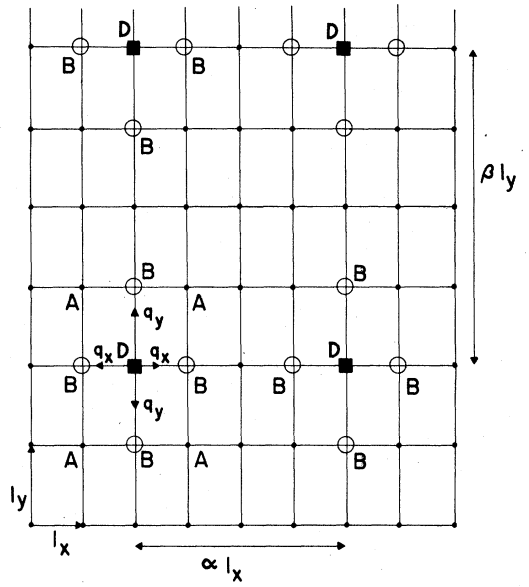

FIG. 1. Random-walk lattice for motion of a single particle on a rectangular lattice with unit cell (l_x, l_y). The total rate to leave a normal site, denoted by ●, is A, with jump probabilities q_x to the right or left and q_y for up and down transitions. Defect sites, denoted by ■, are substitutionally placed, forming a defect superlattice with unit cell $(\alpha l_x, \beta l_y)$. The total rate of leaving a defect site is D. In addition, we consider that the nearest-neighbor sites to defects, denoted by ○, are influenced and have a total rate of leaving of B. Diffusion on several 2D lattices with the same bond lengths and the same defect concentrations and characterizations is compared in the text.

and any other site with rate A. In addition, the defects are arranged periodically with a unit cell of dimension $(\alpha l_x, \beta l_y)$ where α and β are integers larger than 1, and l_x and l_y are the perfect-lattice unit-cell dimensions. The jump probabilities q_x and q_y are not equal in general, and $2(q_x+q_y)=1$. For a square lattice $l_x=l_y$ and $q_x=q_y=\frac{1}{4}$. The transition function $\Psi(\vec{l},\vec{l}';\tau)$ [see Eq. (2.1)] is given by

$$\Psi(\vec{l},\vec{l}';\tau) = [Ae^{-At}(1-\delta_{\vec{l}',\vec{d}}) + (Be^{-Bt}-Ae^{-At})(\delta_{\vec{l}',(\alpha j\pm 1,\beta m)} + \delta_{\vec{l}',(\alpha j,\beta m\pm 1)}) + (De^{-Dt}-Ae^{-At})\delta_{\vec{l}',(\alpha j,\beta m)}]$$
$$\times[q_x\delta_{\vec{l}-\vec{l}',\pm(1,0)} + q_y\delta_{\vec{l}-\vec{l}',\pm(0,1)}] , \tag{3.7}$$

where $\vec{d}$ represents sites with release rates B or D and [See Eq. (I4.10)]

$$\lim_{u\to 0}\Phi(u) = \frac{1}{A} + \frac{1}{\alpha\beta}\left(\frac{4}{B}+\frac{1}{D}-\frac{5}{A}\right). \tag{3.8}$$

Using Eq. (I4.13) with the above, we get

$$\sigma_r^2(t) = 2q_r l_r^2\left[\frac{1}{A} + \frac{1}{\alpha\beta}\left(\frac{4}{B}+\frac{1}{D}-\frac{5}{A}\right)\right]^{-1} \quad (r=x,y). \tag{3.9}$$

Notice that when the effect of the defects is localized to its site (i.e., when $B=A$), and the ratio

between the rates of leaving a defect (D) and a normal site (A) is denoted by $\epsilon = D/A$, then

$$\frac{\sigma_{0,x}^2(t)}{\sigma_x^2(t)} = 1 + \frac{1}{\alpha\beta}\,\frac{1-\epsilon}{\epsilon}, \tag{3.10}$$

where the perfect-lattice diffusion is denoted by $\sigma_{0,x}^2(t) = 2q_x A l_x^2 t$. For defects inhibiting diffusion (i.e., $\epsilon < 1$), $\sigma_0^2(t) > \sigma^2(t)$.

b. Hexagonal lattice. For the hexagonal lattice (see Fig. 2) we use the same designation of rates as described for the square lattice. The periodic unit cell in this case contains four atoms. The transition matrix for the perfect lattice is given by (see Step 4 in Sec. III of Paper I; we follow the labeling in Fig. 2),

$$\underline{\Psi}^{(0)}(\vec{l},t) = \tfrac{1}{3}Ae^{-At}\begin{bmatrix} 0 & \delta_{\vec{l},(0,0)}+\delta_{\vec{l},(1,0)} & 0 & \delta_{\vec{l},(0,-1)} \\ \delta_{\vec{l},(0,0)}+\delta_{\vec{l},(-1,0)} & 0 & \delta_{\vec{l},(0,0)} & 0 \\ 0 & \delta_{\vec{l},(0,0)} & 0 & \delta_{\vec{l},(0,0)}+\delta_{\vec{l},(-1,0)} \\ \delta_{\vec{l},(0,1)} & 0 & \delta_{\vec{l},(0,0)}+\delta_{\vec{l},(1,0)} & 0 \end{bmatrix}. \tag{3.11}$$

From an inspection of Fig. 2 it can be seen that the defect (labeled 3 in the figure) affects three neighboring sites. Two of these (sites 2 and 4) are in the perfect-lattice unit cell (dashed line), while the third one (state 4) is in a neighboring unit cell. Thus the repeating-defect group $\{d\}$ consists of four atoms; the defect (3) and its three neighbors (site 2, and the two equivalent sites, 4). Consequently, the transformed defect matrix for this system is given by Eq. (3.12a)

$$\underline{D}(\vec{k},u) = \frac{1}{3}\begin{bmatrix} 0 & x(B,A)(1+e^{ik_x l_x}) & 0 & 2x(B,A)e^{-ik_y l_y}) \\ 0 & 0 & x(D,A) & 0 \\ 0 & x(B,A) & 0 & 2x(B,A)(1+e^{ik_x l_x}) \\ 0 & 0 & x(D,A)(1+e^{ik_x l_x}) & 0 \end{bmatrix}, \tag{3.12a}$$

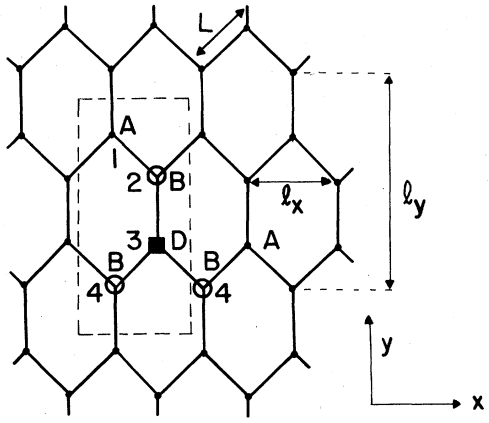

FIG. 2. Random-walk lattice for motion of a single particle on a hexagonal lattice. The bond length is L. Normal (●), defect (■), and nearest-neighbor-to-a-defect (○), sites have total transition rates for leaving of A, D, and B, respectively. Transitions occur with equal probabilities to nearest neighbors. The defect sites (■) form a superlattice with unit cell $(\alpha l_x, \beta l_y)$ where l_x and l_y describe a Cartesian unit cell (dashed lines) with four internal states.

where

$$x(V,W) = V/(V+u) - W/(W+u). \tag{3.12b}$$

Forming the propagator matrix $\underline{R}(k,u) = \underline{M}/\Delta$ [Steps 5 and 6 of the procedure (see Sec. III in Paper I)], and using Eq. (I4.9), we obtain

$$\sigma_x^2 = \frac{tl_x^2}{6}\left[\frac{1}{A} + \frac{1}{4\alpha\beta}\left(\frac{3}{B}+\frac{1}{D}-\frac{4}{A}\right)\right]^{-1} \tag{3.13a}$$

and

$$\sigma_y^2 = \frac{tl_y^2}{18}\left[\frac{1}{A} + \frac{1}{4\alpha\beta}\left(\frac{3}{B}+\frac{1}{D}-\frac{4}{A}\right)\right]^{-1}, \tag{3.13b}$$

where l_x and l_y are the Cartesian distances between equivalent points in neighboring unit cells. Denoting the bond length of the hexagon by L, we may write (see Fig. 2)

$$l_x = \sqrt{3}L, \quad l_y = 3L, \tag{3.14}$$

and thus

$$\sigma_x^2 = \sigma_y^2 = \frac{L^2 t}{2}\left[\frac{1}{A} + \frac{1}{4\alpha\beta}\left(\frac{3}{B}+\frac{1}{D}-\frac{4}{A}\right)\right]^{-1}. \tag{3.15}$$

In order to allow a comparison between diffusion on the square and hexagonal lattices we assume equal bond lengths and equal defect concentrations, which requires that $4(\alpha\beta)_{\text{hexagonal}} = (\alpha\beta)_{\text{square}}$. Under these conditions, equal bond lengths and equal defect concentrations (of defects of type D), it is observed that $\sigma^2_{\text{hex}}(t) > \sigma^2_{\text{sq}}(t)$ if $B > A$, while the reverse holds for $B < A$. Thus, in this example, if the nearest neighbors to defects slow the migration of particles, then the hexagonal lattice is more "immune" to the presence of defects than the square lattice. Note, however, that when $A = B$, $\sigma^2_{\text{hex}}(t) = \sigma^2_{\text{sq}}(t)$. It is only when the range of influence of the defects extends to their neighbors that the effect of structure is exhibited in the diffusion constant.

c. FCC lattice. For particle motion on square fcc lattices of side l we consider nearest-neighbor and next-nearest-neighbor jumps which, are assumed to occur with a probability ratio q_1/q_2. The defects are characterized by a transition rate D for leaving, and its nearest neighbors by a transition rate B. The spacing between equivalent defects is characterized by $(\alpha l, \beta l)$ $(\alpha, \beta$ integers) in the (x, y) directions, (see Fig. 3). Following the procedure demonstrated above for the other lattices we obtain (see Secs. III and IV in Paper I)

$$\lim_{u\to 0} \Phi(u) = \frac{1}{A} + \frac{1}{2\alpha\beta}\left(\frac{4}{B} + \frac{1}{D} - \frac{5}{A}\right) \tag{3.16}$$

and

$$\left.\frac{\partial^2 p(\vec{k})}{\partial k_x^2}\right|_{\vec{k}=0} = q_1 + q_2 = \tfrac{1}{2} - q_1, \tag{3.17}$$

where $4(q_1 + q_2) = 1$ and $0 \leq q_1 \leq \frac{1}{4}$, $0 \leq q_2 \leq \frac{1}{4}$. Finally,

$$\sigma^2_{x,y}(t) = l^2 t(\tfrac{1}{2} - q_1)\left[\frac{1}{A} + \frac{1}{2\alpha\beta}\left(\frac{4}{B} + \frac{1}{D} - \frac{5}{A}\right)\right]^{-1}. \tag{3.18}$$

Note that for vanishing defect concentration, i.e., $(\alpha\beta) \to \infty$ and $q_1 = 0$, the result for a square lattice of side l with no defects is retreived. If $q_1 = \frac{1}{4}$, we obtain the result obtained previously [Eq. (3.9)] for a square lattice of side length $l/\sqrt{2}$. Note that $\sigma^2_{\text{fcc}}(t)$ is always smaller than $\sigma^2_{\text{sq}}(t)$, if both are of the same bond length and there are no defects, since on the fcc lattice one makes jumps of length $l/\sqrt{2}$. In addition, in order to consider equal defect concentrations we must ascribe $2(\alpha\beta)_{\text{fcc}} = (\alpha\beta)_{\text{sq}} = 4(\alpha\beta)_{\text{hex}}$.

d. Triangular lattice. As a final example we consider motion on a defective triangular lattice (Fig. 4), with the same defect characterization as in the previous examples. The defects are arranged in a periodic array, with spacing $(\alpha l_x, \beta l_y)$ in the x and y directions (with l_x, l_y as shown in Fig. 4) and L denoting the bond length of the lattice. Here we obtain

$$\lim_{u\to 0} \Phi(u) = \frac{1}{A} + \frac{1}{2\alpha\beta}\left(\frac{6}{B} + \frac{1}{D} - \frac{7}{A}\right) \tag{3.19}$$

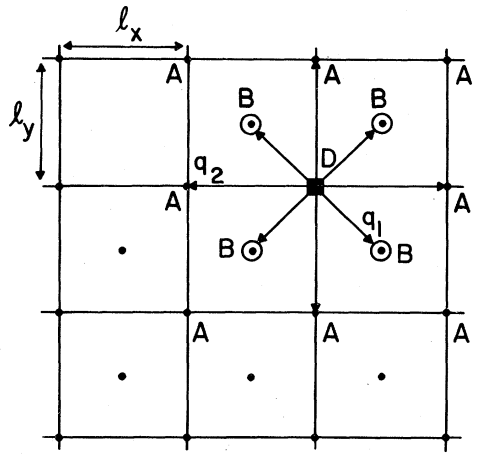

FIG. 3. Random-walk lattice for motion of single particles on a face-centered-square lattice. The total transition rates for leaving normal sites, defect sites, and nearest-neighbor sites are A, D, and B, respectively. The lattice spacing between equivalent normal sites is L. The probability of a transition to a nearest-neighbor site is q_1, and to a next-nearest-neighbor site is q_2. The defect sites (■) form a superlattice with unit cell $(\alpha L, \beta L)$.

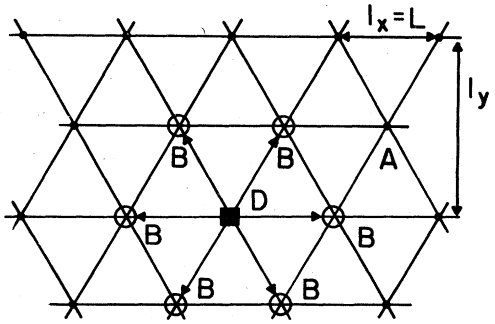

FIG. 4. Random-walk lattice for motion of single particles on a triangular lattice. The bond length is L. The total transition rates for leaving normal, defect, and nearest-neighbor-to-a-defect sites are A, D, and B, respectively. Transitions to nearest neighbors occur with equal probabilities. The defect sites (■) form a superlattice with a Cartesian unit cell $(\alpha l_x, \beta l_y)$ where l_x and l_y describe a unit cell with two states.

and

$$\left.\frac{\partial^2 p(\vec{k})}{\partial k^2}\right|_{\vec{k}=0} = \frac{1}{6}\frac{\partial^2}{\partial k_x^2}[2\cos k_x L + 2\cos(\tfrac{1}{2}k_x + k_y)L + 2\cos(\tfrac{1}{2}k_x - k_y)L]|_{\vec{k}=0} = 3L^2 , \tag{3.20}$$

which yield

$$\sigma^2_{x,y}(t) = \frac{L^2 t}{2}\left[\frac{1}{A} + \frac{1}{2\alpha\beta}\left(\frac{6}{B} + \frac{1}{D} - \frac{7}{A}\right)\right]^{-1} . \tag{3.21}$$

To compare results, at equal defect concentration, with the square lattice it is required that we set $(2\alpha\beta)_{tg} = (\alpha\beta)_{sq}$. For equal defect concentrations and bond lengths we see that if $B \leq A$ then $\sigma^2_{tg} \leq \sigma^2_{sq} \leq \sigma^2_{hex}$, where the equality holds if $B = A$, independent of D.

C. Two-state single-particle diffusion on a defective 2D square lattice

As our next topic we study the diffusion of a particle on a 2D square lattice which contains a periodic array of defects. At each site the particle is assumed to be in one of two states: State 1, in which the particle merely vibrates about the minimum of the potential well associated with that lattice site, and State 2, the mobile state, which the particle achieves by absorbing sufficient energy to surmount the barrier for migration. Such a model was first suggested by Lennard-Jones[7] and analyzed using statistical-mechanical (partition-function) methods. The random-walk lattice for the above model is shown in Fig. 5.

On a normal site the rates of leaving states 1 and 2 are a_{21} and $A = a_{12} + 4a_{22}$, respectively, and the corresponding rates for a defect site are b_{21} and $B = 4b_{12} + 4b_{22}$, respectively [each of the individual rates is taken in the activated form, i.e., $a_{ij} = \alpha_{ij}\exp(-E_{ij}/k_BT)$, $b_{ij} = \beta_{ij}\exp(-\epsilon_{ij}/k_BT)$, $i,j = 1,2$]. By inspection of Fig. 5, we can construct the following Fourier and Laplace transformed defect matrix

$$\underline{D}(\vec{k},u) = \begin{bmatrix} 0 & \dfrac{b_{21}}{B+u} - \dfrac{a_{21}}{A+u} \\ \dfrac{b_{21}}{b_{21}+u} - \dfrac{a_{21}}{a_{21}+u} & 2\left(\dfrac{b_{22}}{B+u} - \dfrac{a_{22}}{A+u}\right)(\cos k_x L + \cos k_y L) \end{bmatrix} . \tag{3.22}$$

Following the steps of the procedure listed above (see Sec. III in Paper I), we obtain for the position variances in the x and y directions

$$\sigma_x^2(t) = \sigma_y^2(t) = 2L^2 t(F/G) , \tag{3.23a}$$

where

$$F = \frac{a_{22}}{A} + (2\beta)^{-1}\left(\frac{b_{22}}{B} - \frac{a_{22}}{A}\right) \tag{3.23b}$$

$$G = \left[\frac{a_{12}}{A} + (\alpha\beta)^{-1}\left(\frac{b_{12}}{B} - \frac{a_{12}}{A}\right)\right] \times \left[\frac{1}{a_{21}} + (\alpha\beta)^{-1}\left(\frac{1}{b_{21}} - \frac{1}{a_{21}}\right)\right] + \frac{1}{A} + (\alpha\beta)^{-1}\left(\frac{1}{B} - \frac{1}{A}\right) . \tag{3.23c}$$

Note that the above result reduces to the ideal-lattice case

$$\sigma_r^2(t) = [2a_{22}a_{21}/(a_{12}+a_{21})]L^2 t \quad (r = x, y) \tag{3.24}$$

for vanishing defect concentration, i.e., $(\alpha\beta) \to \infty$. Also, if the rate of decay from the mobile state (2) to the immobile state (1) vanishes (i.e., $a_{12} = 0$), the result for a state-1 particle is recovered [i.e., $\sigma_r^2(t) = 2a_{22}L^2 t$]. Furthermore, when transitions from the mobile state are dominant (i.e., a_{22}, b_{22} are greater than other rates) and state 2 is highly populated (small activation energy to achieve the mobile state, a_{21} large, and slow rate of decay, a_{12} small),

$$\sigma_r^2(t) = 2a_{22}[1 + (\alpha\beta)^{-1}(a_{22}/b_{22} - 1)]^{-1}L^2 t . \tag{3.25}$$

When the defects act as traps (i.e., $a_{22} > b_{22}$), it is seen that the diffusion is decreased.

D. Dimer migration on 1D and 2D defective lattices

The observation and measurement of the *correlated motion* of adatoms on surfaces (cluster migration) by means of field-ion-microscopy techniques provide information about the adsorbate particle-substrate and interparticle interactions.[4] Such information is of fundamental interest to the understanding of surface adsorption and related phenomena such as thin-film growth, damage annealing, and the mechanisms of certain surface reactions. The surface systems described above may contain defects (and most realistic systems

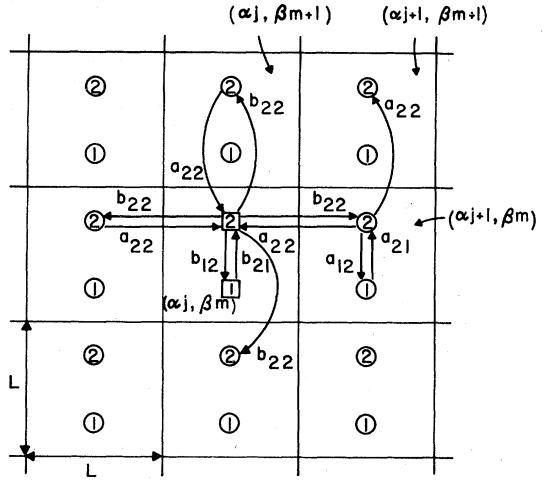

FIG. 5. Random-walk lattice is shown in 2D for single-particle motion where state 1 corresponds to an immobile state and state 2 is an excited mobile state, as first proposed by Lennard-Jones.[7] Defective sites [located at $(\alpha jL, \beta mL)$ for j and m integer] assumed to form a superlattice with unit cell $(\alpha L, \beta L)$ are denoted by squares, while normal sites are denoted by circles. The total transition rate out of a state is the sum of all the transition rates leaving the site, e.g., the total rate of leaving a normal state 2 is $A = 4a_{22} + a_{12}$. The probability of going to a particular site is the rate of going to that site divided by the total rate of leaving, e.g., the probability to go from a normal site 2 to a particular nearest neighbor 2 is a_{22}/A, and that of relaxing to the immobile state 1 on a normal site is a_{12}/A.

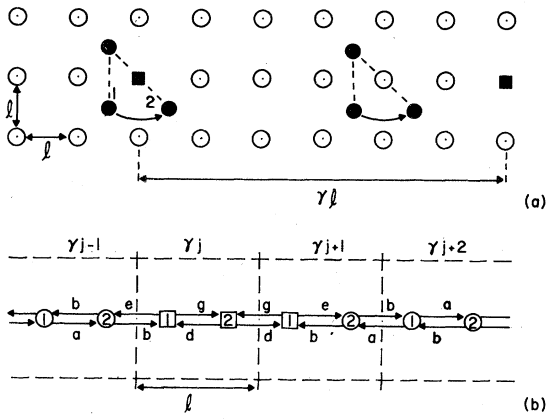

FIG. 6. (a) We illustrate the motion of a dimer (●···●) in 1D with two allowable states: straight (1) and staggered (2). The dimer migrates by alternating between these two states. We consider the effect of substitutional defects (■, located at γjl for integer j) forming a superlattice with unit-cell dimension γl in the x direction. Nondefective sites are denoted by open circles (○). (b) Centroid position of the dimer is mapped onto a random-walk lattice with two states per unit cell. The total transition rates to leave states 1 (straight) and 2 (staggered) are $2a$ and $2b$ respectively, from normal sites, and $g+e$ and $2d$ for defective sites.

will undoubtedly contain defects to various degrees, depending upon operating conditions, sample treatment, etc.) which may exhibit themselves in various ways. Defects may act as inhibitors or promoters of surface migration.[20] In addition, active sites for reactions may also be regarded as defects.[16] Finally, multicomponent surfaces may also be viewed as defective systems. A characterization of particle motion on such surfaces requires the determination of parameters characterizing the motion, of both normal and defective sites.

The migration of adatom clusters on surfaces has been analyzed by us previously,[2,5] yielding expressions which allow the determination of individual transition rates for transitions between cluster configurations involved in the migration mechanism. Here we derive expressions for dimer motion on certain 1D and 2D defective lattices.

a. Channeled motion on a 1D *defective lattice.* As has been observed, on certain crystal faces the motion of adparticles is one-dimensional.[25,4] We consider the 1D motion of an adatom dimer on a substitutional periodic defective lattice (see Fig. 6). The defects are located at γl (γ = integer), and the rates associated with the various transitions are given in the caption to Fig. 6. The real-space motion of the dimer [Fig. 6(a)] has been mapped onto a defective random-walk lattice [see Fig. 6(b)] with two states per unit cell (corresponding to the two dimer configurations). By inspection of Fig. 6(b) we construct the propagator matrix $\underline{R}(\vec{k}, u; z)$ [see Eq. (2.4)]: where

$$H_{\pm}(x;k) = \frac{1}{2}\frac{x}{x+u}(1+e^{\pm ikl}), \tag{3.27}$$

$$I_{\pm}(x_1, x_2; k) = \left(\frac{x_1}{x_1+u} - \frac{x_2}{x_2+u}\right)(1+e^{\pm ikl}), \tag{3.28}$$

$$\underline{1} - \underline{\Psi}^{(0)}(\vec{k}, u) - \frac{1}{\gamma}\underline{D}(\vec{k}, u) = \begin{bmatrix} 1 & -H_+(B;k) - (1/2\gamma)I_+(D,B;k) \\ -H_-(A,k) - (1/\gamma)[J(g,E,e,E) & \\ +J(e,E,g,E) - 2H_-(A,k)] & 1 \end{bmatrix}, \tag{3.26}$$

$$J(x_1,x_2,x_3,x_4;k)=\frac{x_1}{x_2+u}+\frac{x_3}{x_4+u}e^{-ikl}, \qquad (3.29)$$

$A=2a$, $B=2b$, $E=g+e$, and $D=2d$. Using Eq. (I4.9), we find for the variance

$$\sigma^2(t)=\frac{1}{2}l^2t\left[\frac{1}{A}+\frac{1}{B}+\frac{1}{\gamma}\left(\frac{2}{E}+\frac{1}{D}-\frac{2}{A}-\frac{1}{B}\right)\right]^{-1}. \qquad (3.30)$$

Clearly, when the defect concentration vanishes (i.e., $\gamma\to\infty$), the result for the ideal 1D lattice is recovered [see Eq. (3.14) in Ref. 2]. The above expression, coupled with measurement of the probabilities of occupation of the configurational states of the cluster on normal and defect sites, could be used for a complete determination of the parameters characterizing migration in this system.

b. 2D motion of a dimer on a defective lattice. Consider a surface with substitutionally, periodically placed defects, forming a defect superstructure of unit cell $[(\gamma_x l,\gamma_y l)$, where l is the unit-cell dimension of the substrate and γ_x,γ_y are integers]. The real-space motion of the dimer is shown in Fig. 7(a). The dimer centroid performs a random walk on a lattice with three internal states per unit cell [see random-walk lattice in Fig. 7(b)]. The rate of leaving states 1 and 3 is denoted by A, and that of leaving state 2 by B. When a defect is placed in cell $(\gamma_x j,\gamma_y m)$, the transition rates into and out of cells $(\gamma_x j,\gamma_y m)$, $(\gamma_x j+1,\gamma_y m)$, and $(\gamma_x j,\gamma_y m-1)$ are modified. The rate of leaving states 1 and 3 near a defect site is denoted by C, and the rate of leaving state 2 by D. Consequently, the propagator on the ideal lattice is determined from the transition matrix

$$\underline{1}-\underline{\Psi}^{(0)}(\vec{k},u)=\begin{bmatrix}1 & -\frac{1}{2}H_+(B,k_x) & 0\\ -H_-(A,k_x) & 1 & -H_+(A,k_y)\\ 0 & -\frac{1}{2}H_-(B,k_y) & 0\end{bmatrix}. \qquad (3.31)$$

Furthermore,

$$\underline{D}(\vec{k},u)=\begin{bmatrix}0 & -\frac{1}{2\gamma_x\gamma_y}I_+(D,B,k_x) & 0\\ -\frac{1}{\gamma_x\gamma_y}I_-(C,A,k_x) & 0 & -\frac{1}{\gamma_x\gamma_y}I_+(C,A,k_y)\\ 0 & -\frac{1}{2\gamma_x\gamma_y}I_-(D,B,k_y) & 0\end{bmatrix}, \qquad (3.32)$$

and the waiting-time matrix is

$$\lim_{u\to 0}\underline{\Phi}(u)=\begin{bmatrix}A^{-1}+2(\gamma_x\gamma_y)^{-1}(C^{-1}-A^{-1}) & 0 & 0\\ 0 & B^{-1}+(\gamma_x\gamma_y)^{-1}(D^{-1}-B^{-1}) & 0\\ 0 & 0 & A^{-1}+2(\gamma_x\gamma_y)^{-1}(C^{-1}-A^{-1})\end{bmatrix}. \qquad (3.33)$$

Using the results in Paper I [Eq. (I4.8)], we obtain

$$\sigma_r^2(t)=\frac{l^2t}{4}\left[\frac{1}{A}+\frac{2}{\gamma_x\gamma_y}\left(\frac{1}{C}-\frac{1}{A}\right)+\frac{1}{\gamma_x\gamma_y}\left(\frac{1}{D}-\frac{1}{A}\right)+\frac{1}{B}\right]^{-1}, \qquad (3.34)$$

where $(r=x,y)$. Again, for vanishing defect concentrations (i.e., $\gamma_x\gamma_y\to\infty$), the result for motion on a perfect lattice is recovered [see Eqs. (3.24) and (3.25), with $d=a$, in Ref. 2].

IV. MECHANISMS OF VACANCY DIFFUSION

In this section we apply our formalism to the investigation of transport via vacancy mechanisms in crystalline materials. A most useful method for the measurement of diffusion in solids is via the radio tracer technique.[8-11] In this method a thin layer of a radio tracer is deposited on the surface of the solid and the specific activity of the tracer monitored as a function of distance from the surface is measured by successive sectioning of the solid. For these experimental conditions the solution to the diffusion equation is

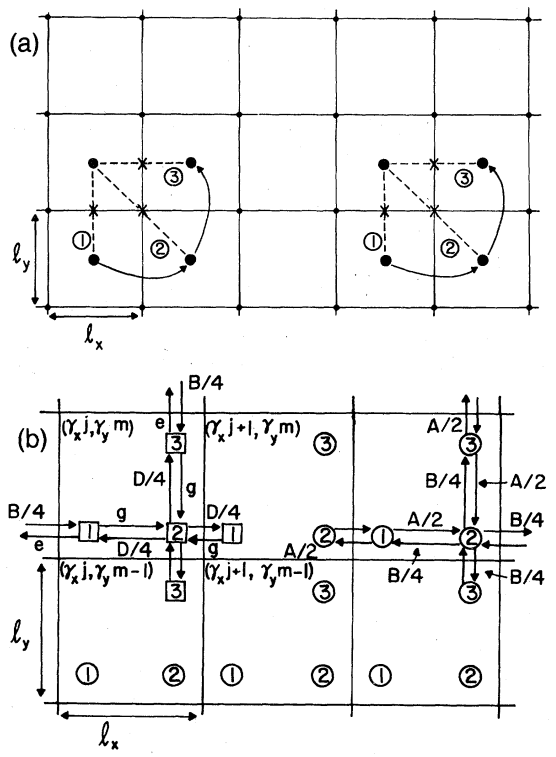

FIG. 7. (a) Two-dimensional dimer migration. (a) Three possible spatial configurations of a dimer (large filled circles connected by a dashed line) on a square 2D lattice (small filled circles). The position of the dimer centroid is denoted by a cross (×). The allowed equivalent mirror-image configurations are not shown. Transitions involving a defect (denoted by a filled square) are shown on the left. (b) Random-walk lattice corresponding to the centroid motion indicated in (a). States affected by the defect [whose location is at $(\gamma_x jl, \gamma_y ml)$] are denoted by squares to distinguish from those which are normal, denoted by circles. The arrows denote allowed transitions and are labeled by the transition rates. The total rate for leaving normal states 1 and 3 is A, and that of leaving a normal state 2 is B. The corresponding total rates for transitions involving a defect are $C = g + e$ for leaving states 1 and 3, and D for leaving state 2.

$$C(x) = [S/(\pi Dt)^{1/2}]e^{(-x^2/4Dt)}, \qquad (4.1)$$

where $C(x)$ is the specific activity of the tracer at distance x from the surface, t is the time of anneal, S is the tracer concentration per unit area at $x = 0$ and $t = 0$, and D is the sought-after diffusion coefficient. Performing such measurements for a number of temperatures T, we obtain a plot of the diffusion coefficient vs $1/T$. If the diffusion coefficient is of a simple Arrhenius form ($D = D_0 e^{-E/k_B T}$) the above plot will yield a straight line whose slope and intercept are E/k_B and D_0, respectively.

Over the past decade it has been observed that self-diffusion in a number of metals (both bcc and fcc) exhibits *non-Arrhenius* curved behavior[8-11] in certain temperature ranges. The two models which have been suggested for explaining curved Arrhenius plots in diffusion measurements are: (i) temperature dependence of enthalpy and entropy of defect formation and migration,[10] and (ii) a combination of single-vacancy and divacancy migration mechanisms.[8,9,11] Following the second model, phenomenological two-exponential fits (or three-exponential when an additional interstitial mechanism is included) to the data have been attempted, yielding adequate agreement.

Recent molecular-dynamics studies[26] of transport in Na (bcc) and Al (fcc) have shown the occurrance of *three monovacancy mechanisms:* single jumps (SJ), where the atom migrates to a nearest-neighbor vacancy; second-nearest-neighbor jumps (SNNJ), where an atom migrates to a second-nearest-neighbor vacancy; and double jumps (DJ) where two atoms, one nearest-neighbor and the other second-nearest neighbor to a vacancy, perform colinear jumps within a very short time delay, thus leading to a double jump of the vacancy to a non-nearest-neighboring site. In this numerical study, the weighted contribution from these three migration mechanisms (which varies with temperature) has been suggested as the origin of the "anomalous" non-Arrhenius curved behavior of the diffusion coefficient. Following the above results, we model the diffusion as a random walk with three states (states 1, 2, and 3 corresponding to SJ, DJ, and SNNJ, respectively) and evaluate an analytical expression for the diffusion coefficient. As we proceed to show, the diffusion coefficient which we derive does exhibit non-Arrhenius behavior. Note, that the model consists of *competing monovacancy mechanisms* and *does not invoke* the occurance of divacancies or other species (this does not rule out, however, the possibility of contributions from divacancies or from an inherent temperature dependence of the activation energies and frequency factors).

Consider a simple cubic (sc) lattice containing a vacancy. The filling of the vacancy may occur via three possible mechanisms of particle migration: SJ, DJ, and SNNJ, which we designate as the three states of the vacancy (1, 2, and 3). Each of the above processes (states) involves a different type of atomic motion; thus they are characterized by different transition rates a_{ji} [$a_{ji} = \nu_{ji} \times e^{-E_{ji}/k_B T}$] with different preexponential and activation energies. The probability that the vacancy be found in any of the three possible states (i.e., that any of the three atomic migration

processes occur) is determined by the rates $a_{21} = \nu_{21} e^{-E_{21}/k_B T}$ and $a_{31} = \nu_{31} e^{-E_{31}/k_B T}$ and thus the contribution from DJ and SNNJ depends upon the corresponding activation energies and frequency factors and on temperature. Once in states 2 or 3, migration occurs via a DJ or a SNNJ, with transition rates b_{12} or c_{13}, respectively. We will assume (with no loss of generality) these transition rates (b_{12}, c_{13}) to be large, so that the diffusion mechanism is determined by the rates a_{21} and a_{31} for populating the DJ and SNNJ states, and the rate of performing SJ's $a_{11} = \nu_{11} e^{-E_{11}/k_B T}$. By inspection of the random-walk lattice (Fig. 8) we construct the transition matrix for the model:

$$\underline{\Psi}(\vec{k}, u) = \begin{bmatrix} \frac{2a_{11}}{A+u} C_1 & \frac{2b_{12}}{B+u} C_2 & \frac{2c_{13}}{C+u} C_3 \\ \frac{a_{21}}{A+u} & 0 & 0 \\ \frac{a_{31}}{A+u} & 0 & 0 \end{bmatrix}, \tag{4.2}$$

where

$$A = 6a_{11} + a_{21} + a_{31}, \tag{4.3a}$$

$$B = 6b_{12}, \tag{4.3b}$$

$$C = 12c_{13}, \tag{4.3c}$$

$$C_1 = \cos k_x l + \cos k_y l + \cos k_z l, \tag{4.4a}$$

$$C_2 = \cos 2k_x l + \cos 2k_y l + \cos 2k_z l, \tag{4.4b}$$

$$C_3 = \cos(k_x l + k_y l) + \cos(k_x l + k_z l) + \cos(k_y l + k_z l) + \cos(k_x l - k_y l) + \cos(k_x l - k_z l) + \cos(k_y l - k_z l), \tag{4.4c}$$

where l is the unit-cell dimension.

Using the waiting-time matrix $\underline{\Psi}(\vec{k}, u)$, we construct the propagator matrix $\underline{R} = \underline{M}/\Delta$ [see Eq. (2.4) and Step 6 in Sec. III of Paper I]. The determinant Δ can be written as

$$\Delta = 1 - \frac{2a_{11}}{A+u} C_1 - \frac{2a_{21}b_{12}}{(A+u)(B+u)} C_2 - \frac{2a_{31}C_{13}}{(A+u)(C+u)} C_3 .$$

Following the method described in detail in Eq. (I4.9b), we write the variance as

$$\sigma_r^2(t) = tl^2 \lim_{u \to 0} \left(\Delta_0^{-1} \frac{\partial^2 \Delta}{\partial k_r^2} \right)_{\vec{k}=0},$$

where Δ_0 is defined in Eq. (I4.6). The above yields a general expression for the variance in position for vacancy diffusion in a *sc* lattice

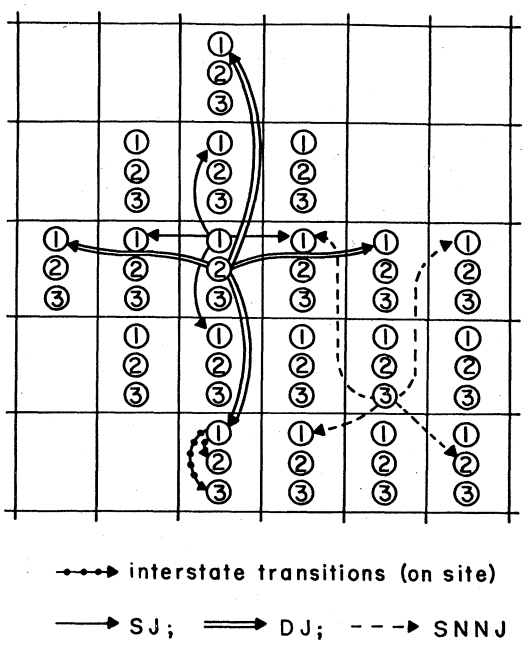

FIG. 8. Motion of a monovacancy mapped onto a random-walk lattice (2D section of a sc lattice is shown) with three states per unit cell. State 1 corresponds to an uncorrelated single atomic jump (SJ) into a vacancy (single arrow). State 2 corresponds to two atoms jumping colinearly, and nearly simultaneously, leading to a double jump (DJ) of the vacancy (double arrows). State 3 corresponds to a single nearest-neighbor jump (SNNJ) (dashed arrow). After any type of jump we assume that the system relaxes immediately to state 1. If the rate-limiting step is the transition from state 1 to states 1, 2, or 3 (with rates a_{11}, a_{21}, and a_{31}, respectively), then the resulting expression for the monovacancy diffusion constant is a weighted sum of three terms, each of which is an exponential if the transition rates are activated (i.e., $a_{ij} = \nu_{ij} e^{-E_{ij}/kT}$). The resulting expression describes the non-Arrhenius behavior of vacancy diffusion near the melting temperature.

$$\sigma_r^2(t) = t \frac{2a_{11}BC + \frac{4}{3}a_{21}BC + \frac{2}{3}a_{31}BC}{a_{21}C + a_{31}B + BC} .$$

If the rates a_{11}, a_{21}, and a_{31} are the rate-limiting steps (i.e., if the corresponding processes are slower than other processes in the model), the following expression is obtained:

$$\sigma_r^2(t) = l^2 t (2\nu_{11} e^{-E_{11}/k_B T} + \tfrac{4}{3}\nu_{21} e^{-E_{21}/k_B T} + \tfrac{2}{3}\nu_{31} e^{-E_{31}/k_B T}), \tag{4.5}$$

for $r = x, y, z$. Similarly, for a bcc solid we find

$$\sigma_r^2(t) = l^2 t (2\nu_{11} e^{-E_{11}/k_B T} + \nu_{21} e^{-E_{21}/k_B T} + \tfrac{1}{3}\nu_{31} e^{-E_{31}/k_B T}), \tag{4.6}$$

and for a fcc solid

$$\sigma_r^2(t) = l^2 t(2\nu_{11}e^{-E_{11}/k_BT} + \tfrac{2}{3}\nu_{21}e^{-E_{21}/k_BT} + \tfrac{1}{3}\nu_{31}e^{-E_{31}/k_BT}) . \quad (4.7)$$

It is seen from the above that a three-exponential expression is obtained for the variance in position. However, we did not invoke the occurance of new species (like divacancies or interstitials), deriving our results on the basis of *competing monovacancy mechanisms only*. The relative contributions of the three processes involved depend upon the relative magnitudes of the characteristic activation energies and frequency factors [(ν_{11}, E_{11}) for SJ, (ν_{12}, E_{21}) for DJ, and (ν_{31}, E_{31}) for SNNJ], and upon the temperature. In certain temperature ranges, the contributions from two or more terms may become significant and deviations from a linear Arrhenius behavior will occur. It should be noted that the diffusion coefficients derived above are for the vacancy motion. The particle (radio-tracer) diffusion D_p is related to that of the vacancy D_v by[27]

$$D_p = ([v]/[p])D_v f ,$$

where $[v]$ and $[p]$ are the vacancy and particle concentrations and f is the correlation-function factor. Thus the results obtained in the above can be used in the analysis of radiotracer diffusion measurements.

V. TIME-DEPENDENT CORRELATED MOTION

Microscopic models of mechanisms of particle transport in solids are characterized by certain time constants. These time constants are related to the dynamic response of the solid (vibrational frequencies, local-mode frequencies, saddle-point crossing frequencies, and lattice relaxation times). The relative magnitudes of the characteristic time constants determine the contributions of the corresponding modes of response of the lattice to the transport mechanism. Consider an activated migration of a particle between two equivalent sites (1 and 2) in a solid. Starting at site 1, the outcome of the migration step is when the particle attains site 2. In the process of particle migration the host lattice may deform from its equilibrium configuration. The return of the system to its initial equilibrium configuration is governed by a relaxation time T_1. In the event that the time delay between particle jumps (T_2) is larger than the lattice relaxation time (T_1), each particle transition is uncorrelated from its previous one. However, when $T_1 > T_2$, a transition of the particle will be correlated to its previous position, and thus the stochastic evolution of the particle position is non-Markovian. We emphasize that the dynamic correlation effects discussed in this section should not be confused with the spatial correlation associated with the motion of a cluster, discussed in Sec. III. Correlations of the type discussed here may occur in particle or excitation (e.g., polaron) migration in condensed-matter systems. The effect of such correlations on quasielastic neutron scattering line shapes is discussed in Sec. VI.

Correlated random walks where time is not involved and where *only* the *statistics* of the random-walk path is considered have been studied previously.[28-33] If the system is not allowed to return to its previous state on the next transition then the problem is that of a random walk with a restricted reversal. A generalization of this correlated random walk is a forbidden return to a previous state after a finite number of suceeding transitions. These types of problems have been treated first by Montroll[28] and later by others[29-33] as approximations to the restricted random walk of polymer configurations where no polymer units may overlap.

In the following we illustrate the application of our formalism to the study of correlated motions. We consider a one-dimensional motion which is mapped onto a random-walk lattice with two internal states per unit cell (see Fig. 9). The particle achieves state 1 on site j when the transition is from the $j-1$ site. When the jth site is occupied by a transition originating from site $j+1$, state 2 is obtained. Associated with the above two states are the transition probabilities: $q(t)$ for return to the site where the previous jump originated and $p(t)$ for propagation in the other direction. These transition probabilities are assumed to be of the form

$$p(t) = \tfrac{1}{2} + \epsilon e^{-t/T_1} , \quad (5.1)$$

$$q(t) = \tfrac{1}{2} - \epsilon e^{-t/T_1} , \quad (5.2)$$

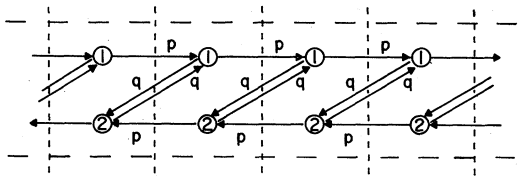

FIG. 9. Correlated non-Markovian motion of a random walker in 1D mapped onto a lattice with two states in each unit cell (dashed lines); state 1 corresponds to the event that the lattice site was occupied as a result of a transition from the left and is distinguished from state 2, which is occupied when the transition to this lattice site was from the right. The probability of the next jump being in the same direction as the preceding one is denoted by p, and in the reverse direction it is denoted by q. The generalization to correlations over more than the preceding jump involve additional internal states.

where ϵ is a constant (positive or negative) such that $p(t)$ and $q(t)$ are smaller than unity. In the limiting case that the average time between particle jumps T_2 is much smaller than the characteristic lattice relaxation time T_1, the transition probabilities reduce to

$$p = \tfrac{1}{2} + \epsilon\,, \quad q = \tfrac{1}{2} - \epsilon\,. \tag{5.3}$$

If, on the other hand, the reverse holds (i.e., $T_2 \gg T_1$), $p = q = \frac{1}{2}$, and the motion is uncorrelated.

The transition matrix for the above model is given by

$$\underline{\Psi}(l,t) = \frac{1}{T_2}\, e^{-t/T_2} \begin{pmatrix} p(t)\delta_{l,1} & q(t)\delta_{l,1} \\ q(t)\delta_{l,-1} & p(t)\delta_{l,-1} \end{pmatrix}. \tag{5.4}$$

The inverse of the transformed propagator, $\underline{R}(k,u) = [\underline{1} - \underline{\Psi}(k,u)]^{-1}$, is given by

$$[\underline{R}(k,u)]^{-1} = \frac{1}{\Delta} \begin{pmatrix} 1 - x_+(u)e^{-ik} & -x_-(u)e^{+ik} \\ -x_-(u)e^{-ik} & 1 - x_+(u)e^{+ik} \end{pmatrix}, \tag{5.5}$$

where Δ is the determinant of the matrix $\underline{1} - \underline{\Psi}(k,u)$, and

$$x_\pm(u) = \frac{1}{2}\,\frac{1/T_2}{1/T_2 + u} \pm \epsilon\,\frac{1/T_2}{1/T_1 + 1/T_2 + u}. \tag{5.6}$$

Using Eq. (2.10a) of Ref. 2, we get

$$\sigma^2(t) = \sum_{j=1}^{2}\sum_{j'=1}^{2} \mathfrak{L}^{-1}\left(\left.\frac{\partial^2 R_{jj'}(\vec{k},u)}{\partial k^2}\right|_{k=0} \times u^{-1}[1 - \psi_j(u)] \right) p_{j'}\,, \tag{5.7}$$

where $p_{j'}$ is the initial probability that the particle will occupy state j' ($p_1 = p_2 = \frac{1}{2}$ in the present case), thus accounting for the two alternative ways in which the particle starts its walk at $t = 0$. Expressing $\underline{R}(k,u) = \underline{M}/\Delta$ and using Eq. (2.24) of Ref. 2, we obtain the general result

$$\sigma^2(t) = \frac{l^2}{T_2}\,\frac{1 + 2\epsilon + T_2/T_1}{1 - 2\epsilon + T_2/T_1}\,t + \frac{1 - e^{-E_- t}}{E_-}\left(1 - \frac{E_+}{E_-}\right), \tag{5.8}$$

where

$$E_\pm = 1/T_1 \pm (1 + 2\epsilon)/T_2\,. \tag{5.9}$$

In the above expression the first term dominates in the long-time (diffusion) limit.

For an uncorrelated walk ($\epsilon = 0$ or $T_1 \ll T_2$), the expression for the variance reduces exactly to $\sigma_0^2(t) = l^2 t/T_2$, which is the known result for simple-particle diffusion on a 1D lattice. In the opposite limit, for a system where particle jumps occur before the lattice relaxes ($T_1 \gg T_2$), we obtain

$$\sigma^2(t) = \sigma_0^2(t)\frac{p}{q} + \frac{l^2}{2q}\left(1 - \frac{p}{q}\right)(1 - e^{-2qt/T_2}). \tag{5.10}$$

Note that in the limit of $q \to 0$ (i.e., immediate return to the previously occupied site is negligible) the variance in position is given by

$$\sigma^2(t) \sim (p/T_2^2) l^2 t^2 + O(qt^3)\,, \tag{5.11}$$

which is not of diffusion character [i.e., $\sigma^2(t) \propto t$]. However, for time $t \gg T_2/2q$, the first term in Eq. (5.10), which is of diffusion character, dominates.

VI. QUASIELASTIC NEUTRON SCATTERING FROM DIFFUSING SPECIES

Neutron scattering is a powerful method for obtaining information about the structure and dynamics of liquids and solids.[34] The theoretically sharp elastic zero-energy transfer line ($\hbar\omega = 0, \hbar\vec{k} \neq 0$) is broadened by diffusive motion, yielding the quasielastic neutron scattering line shape $S(\vec{k},\omega)$, where $\hbar\omega$ and $\hbar\vec{k}$ are the energy and momentum transfers. This line shape contains contributions from coherent scattering from many different atoms and incoherent scattering from individual atoms. For certain systems (e.g., hydrogen in metals such as niobium[35]) the large incoherent scattering cross section dominates the coherent one. We will be interested in the incoherent quasielastic neutron scattering (QNS) because it can yield information about transition rates, diffusion constants, and structural positions of migrating interstitials in solids. A similar analysis also applies to the diffusionally broadened Mössbauer resonant absorption line.[36]

The incoherent scattering law was derived by Van Hove[37] in the form

$$S(\vec{k},\omega) = \frac{1}{2\pi}\int\int e^{i(\vec{k}\cdot\vec{r} - \omega t)} G(\vec{r},t)\, d\vec{r}\, dt\,, \tag{6.1}$$

where G is a quantum correlation function. In the high-temperature limit ($k_B T > \hbar\omega$) $G(\vec{r},t)$ becomes[38,39] the classical correlation function for a particle to be at position $\vec{r}$ at time t if it was at $\vec{r} = 0$ initially. This approximation holds for times of $t \gtrsim 10^{-13}$ sec. In our analysis the classical approximation will be employed.

For simple diffusion of a particle in a 3D sc lattice where the particle makes transitions with a rate a and with equal probability to its neighbors a Lorentzian line shape is obtained[34] for $S(k,\omega)$:

$$S(\vec{k},\omega)=(1/\pi)\,p(\vec{k})/[p^2(\vec{k})+\omega^2]\,, \tag{6.2}$$

where

$$p(\vec{k})=\tfrac{1}{3}a(3-\cos k_x l_y-\cos k_y l_y-\cos k_z l_z)\,.$$

In the limit of small momentum transfer $\vec{k}$, Eq. (6.2) becomes $S(\vec{k},\omega)=(1/\pi)\Gamma(\Gamma^2+\omega^2)^{-1}$, where $\Gamma=Dk^2$, with the diffusion coefficient D for a sc lattice equal to $\frac{1}{6}al^2$.

We can determine the rate a by

$$\lim_{\vec{k}\to 0}\pi S(\vec{k},\omega=0)k^2=a\,. \tag{6.3}$$

Thus a plot of $S(\vec{k},\omega=0)$ vs $(\pi k^2)^{-1}$ for small $\vec{k}$ yields the transition rate a. In practice, the diffusion constant D is extracted from data for the width of the scattering cross section $S(\vec{k},\omega)$ as a function of k^2.

The most studied system with QNS is the diffusion of hydrogen in metals.[35,40] It has been observed that the data is non-Lorentzian and usually cannot be explained by the predictions of simple jump models.[40] Thus more sophisticated diffusion mechanisms and models are needed.[40,41] We give here a general formula for $S(\vec{k},\omega)$ which includes the effects of internal states, clusters, correlations, and periodic defects. We emphasize that only for the simple example given above [Eq. (6.2)] does a single Lorentzian line shape occur. In other systems, the dynamics of the system (i.e., correlations, cluster motion, and internal states) and the heterogeneous character of the medium (defects) would manifest themselves as deviations from a single Lorentzian line shape.

From Eq. (6.1), in the classical limit, we obtain

$$S(\vec{k},\omega)=\frac{1}{\pi}\mathrm{Re}\sum_{m,n}\int d\vec{r}\int_0^\infty dt\, e^{i(\vec{k}\cdot\vec{r}-\omega t)}\times P_{mn}(\vec{r},t\,|\,\vec{r}=0,t=0)p_n \tag{6.4a}$$

$$=\frac{1}{\pi}\mathrm{Re}\sum_{m,n}P_{mn}(\vec{k},i\omega)p_n$$

$$=\frac{1}{\pi}\mathrm{Re}\sum_{m,n}R_{mn}(\vec{k},i\omega)\left(\frac{1-\psi_{mm}(i\omega)}{i\omega}\right)p_n\,, \tag{6.4b}$$

where we have averaged over initial positions n and summed over final ones m.

Let us consider first the case of single-particle motion in 1D with temporal correlation, discussed in the previous section. We limit our discussion to the case of $T_1\gg T_2$, i.e., the transition probabilities are $p=\frac{1}{2}+\epsilon$ and $q=\frac{1}{2}-\epsilon$ [see Eq. (5.3)]. For this case the matrix $\underline{R}(k,u)$ given in Eq. (5.5) reduces to (with k in units of inverse lattice spacing)

$$\underline{R}(k,u)=\Delta^{-1}\begin{pmatrix}1-\frac{\lambda}{\lambda+u}pe^{-ik} & \frac{\lambda}{\lambda+u}qe^{ik}\\ \frac{\lambda}{\lambda+u}qe^{-ik} & 1-\frac{\lambda}{\lambda+u}pe^{ik}\end{pmatrix}, \tag{6.5}$$

where $\lambda\equiv 1/T_2$ and Δ is given as

$$\Delta=1-2p\frac{\lambda}{\lambda+u}\cos k+\left(\frac{\lambda}{\lambda+u}\right)^2(p-q)\,. \tag{6.6}$$

The term in large parentheses in Eq. (6.4b), for an exponential waiting-time distribution $\psi(t)=\lambda e^{(-\lambda t)}$, is given by

$$\Phi_{mm}(i\omega)=(\lambda+i\omega)^{-1} \tag{6.7}$$

for $m=1,2$. The initial-state occupation probabilities are taken to be equal, i.e., $p_1=p_2=\frac{1}{2}$. Substituting into Eq. (6.4b), we obtain

$$S(k,\omega)=\frac{\lambda(1-2\epsilon\cos k)\{\lambda^2[1+2\epsilon-(1+2\epsilon)\cos k]-\omega^2\}+2\lambda\omega^2[1-(\frac{1}{2}+\epsilon)\cos k]}{\{\lambda^2[1+2\epsilon-(1+2\epsilon)\cos k]-\omega^2\}^2+\{2\lambda\omega[1-(\frac{1}{2}+\epsilon)\cos k]\}^2}\,. \tag{6.8}$$

In the event of no temporal correlation $\epsilon=0$, the above result reduces to a Lorentzian [see Eq. (6.2)], and

$$S(k,\omega)=\frac{1}{\pi}\frac{\lambda(1-\cos k)}{[\lambda(1-\cos k)]^2+\omega^2}\,. \tag{6.9}$$

Haus and Kehr[42] have studied temporal correlated motion, deriving coupled rate equations for $P_{mn}(k,\omega)$.

For a system with a periodic arrangement of defects, an expression for $S(\vec{k},\omega)$ given in Eq. (6.4a) may be written explicitly. Using the expression on the right-hand side of Eq. (I2.37) [with $n=0$ and without the indicated inverse Laplace transformation for $P_{ij}(\vec{k},\omega)$], we find for small ω

$$S(\vec{k},\omega)=\frac{1}{\pi}\mathrm{Re}\sum_{m,n}[\underline{\Phi}^{(0)}(i\omega)+\Omega(\underline{\Phi}(i\omega)-\underline{\Phi}^{(0)}(i\omega))]_{mm}\{[(\underline{R}^{(0)}(\vec{k},i\omega)^{-1}-\Omega\underline{D}(\vec{k},i\omega)]^{-1}\}_{mn}p_n\,. \tag{6.10}$$

The above expression is appropriate for small k values, and is useful for analysis of the diffusive behavior from QNS measurements. Study of details of the motion in localized regions such as the vicinity of defects requires an analysis of $S(\vec{k},\omega)$ for large k values, which can be accomplished by employing in the derivation of $S(\vec{k},\omega)$ the full propagator, which contains contributions from k's lying in all the Brillouin zones of the defect superlattice [see Eqs. (I2.21)–(I2.23)].

As an application of Eq. (6.10), consider the QNS from an interstitial whose motion is on a sc lattice with periodic defects, such as has been discussed for the case of hydrogen diffusion in niobium containing nitrogen traps.[40(b)] We assume that the interstitial leaves normal sites with a rate a and defect sites with a rate d, and that the defect superlattice has a unit-cell volume of Ω^{-1}. Then

$$\Phi^{(0)}(i\omega)=(a+i\omega)^{-1},\quad \Phi(i\omega)=d+i\omega\,,$$

$$D(\vec{k},i\omega)=d/(d+i\omega)-a/(a+i\omega)\,,$$

$$\psi^{(0)}(\vec{k},\omega)=a(a+i\omega)^{-1}\tfrac{1}{3}(\cos k_x l_x+\cos k_y l_y+\cos k_z l_z)\,.$$

Substituting into Eq. (6.10), we find as $\omega\to 0$

$$S(\vec{k},\omega)=\pi^{-1}Q^{-1}(\vec{k},\omega)(\{\Omega(a-d)+d\}\{ad[1-C(\vec{k})]-\omega^2\}+\omega^2\{a+d-C(\vec{k})[a-\Omega(a-d)]\}), \tag{6.11}$$

where

$$Q(\vec{k},\omega)=\{ad[1-C(\vec{k})]-\omega^2\}^2+\omega^2\{a[1-C(\vec{k})(1-\Omega)]+d[1-C(\vec{k})\Omega]\}^2$$

and

$$C(\vec{k})=\tfrac{1}{3}(\cos k_x l_x+\cos k_y l_y+\cos k_z l_z)\,.$$

Note that for $a=d$ we recover the Lorentzian line shape. The elastic line ($\omega=0$) yields

$$S(\vec{k},0)=\pi^{-1}[d+\Omega(a-d)]/ad[1-C(\vec{k})]\,. \tag{6.12}$$

If the rate a is known from a system without defects, then the rate d of leaving a defect can be calculated from Eq. (6.12).

To obtain the diffusion constant, a measurement of the scattering intensity versus energy transfer of the scattered particle, for fixed momentum transfer and temperature is performed, and the full width at half-maximum (FWHM) is determined. Obtaining such data for a number of k values, we can make a plot of FWHM vs k^2. Subsequently, one attempts to best fit the experimental observations by choosing the optimal set of parameters in the theoretical expression (for the simple Lorentzian diffusion case a plot of Γ vs k^2 yields a straight line with slope D). Also, measurements at different temperatures could be used in order to obtain the activation energy E_a and frequency factor ν_a for the diffusion. In the case of a single-state diffusion mechanism in a defect-free medium such measurements yield a straight line (of slope $-E_a$ and intercept ν_a) in a plot of $\ln(\Gamma/k^2)$ vs $1/k_BT$. However, for multistate diffusion, correlated motion, and in the presence of defects, the above simple method of analysis is not adequate to fit the data and determine the characteristic diffusion parameters. In these circumstances one must best fit the experimental results with theoretical expressions derived from complex diffusion mechanisms.

The detailed analysis of the incoherent scattering law $S(\vec{k},\omega)$ for diffusion systems where the diffusants may be dimers or other clusters, may have various internal states (e.g., mobile and immobile), may have transitions correlated to previous ones, and in the presence of various types of defects, will be reported by us.

VII. TRANSITION RATES

In all the above examples from FIM, vacancy diffusion, correlated motion, and QNS we have calculated experimentally observable quantities (diffusion distances, occupation probabilities of different internal states, and line shapes) in terms of assigned transition rates. We have given several explicit examples and indications of how to invert the data [Eqs. (3.2), (3.30), (6.3), and (6.12)] to find the individual transition rates between the internal states of the system under study. In general, if there are N transition rates then one needs N equations to fully determine the individual rates. If there are M internal states then $M-1$ detailed balance relations can be found. The other $N-M+1$ equations may be found by considering diffusion distances or line-shape parameters. Other independent equations may be used, when appropriate, to describe the data for NMR, Mössbauer, and various reaction experiments. If there are more possible equations than transition rates then consistency checks can be made. It is also possible that there are more transition rates

than can be determined from the data. For example, consider a dimer which can exist in three states[2] (straight, staggered, and extended staggered) undergoing a 1D motion on a surface. There are four transition rates connecting the three states. Detailed balance relations between the three states yield two equations, and the positional variance of the dimer centroid a third. It is readily seen that an experiment with an electrical bias to polarize the adatoms and favor motion in one direction is necessary to yield a fourth equation for the centroid mean position, which then allows a determination of the four transition rates. Thus the degree of microscopicity one wishes to obtain will determine the type of experiment that should be performed. In addition, the data must be plotted in a proper manner. For example, if one, say for FIM data, simply plots the logarithm of the variance of the centroid position of a cluster vs $1/k_BT$, the individual transition rates cannot be determined and the plot will yield a curved non-Arrhenius line because more than one transition rate is involved. Although in a limited temperature range the curve may appear to be straight, its slope and intercept do not characterize the individual transition rates between the states of the dimer. Thus further information, such as detailed balance relationships as a function of temperature and perhaps the mean motion from experiments under electric basis will be necessary to calculate individual transition rates.

VIII. PROSPECTIVES

In the present study we have employed mappings of diverse transport systems and mechanisms onto random-walk lattices with internal states and defects. The systems and phenomena which we have discussed are: (i) single-particle and dimer motion in one and two dimensions on periodically defective lattices, as observed in field-ion-microscopy experiments. (ii) Multistate diffusion of a single particle in a two-dimensional defective lattice. (iii) The lattice-structure dependence of the diffusion constant for single particles on defective lattices. (iv) The non-Arrhenius behavior of the vacancy diffusion constant in certain metals, as observed in radio-tracer experiments. (v) The effect of temporal correlation on the diffusion constant. (vi) The effect of defects, multistate mechanisms, and temporal and spatial correlations on the quasielastic neutron scattering law $S(\vec{k}, \omega)$. The solutions of the time development of the systems considered were obtained in a unified fashion via a matrix Green's-function propagator (to include internal states) which is renormalized by the presence of defects.

Other systems in which transport is an essential step and to which our formalism can be applied are certain unimolecular and bimolecular reaction systems. Examples include annealing of point defects,[43] electron scavenging in aqueous radiation chemistry,[44] one-way flux of tracer ions through nerve membrane during action potentials,[45] positron[46] and muon[47] trapping in solids, exciton trapping and fusion,[48] and bimolecular heterogeneous reactions of the Langmuir-Hinshelwood mechanism, catalyzed by active sites.[16]

In the latter reactions, adsorbed reactants migrate on a surface and reaction occurs upon the coincidence of two reactants at an active site. The reactants may possess internal states (energetic, spin, orientational, etc.) which may determine the reaction probability upon coincidence. The surface may contain defects other than the active sites, such as migration promotors and inhibitors. The calculation of the rate of reaction proceeds via a stochastic formalism, yielding expressions for the probability distribution of reactive coincidences at active sites. The random-walk propagators for the reactants were discussed in Paper I. Our results show surface structural dependence of the reaction rates and their variation with active-site concentration. We will publish these results[16] and other reaction schemes in due course.

ACKNOWLEDGMENT

Work supported by U.S. DOE Contract No. EG-77-S-05-5489.

[1] C. P. Flynn, *Point Defects and Diffusion* (Oxford University, London, 1972).
[2] U. Landman and M. F. Shlesinger, Phys. Rev. B 16, 3389 (1977).
[3] U. Landman, E. W. Montroll, and M. F. Shlesinger, Proc. Nat. Acad. Sci. U. S. A. 74, 430 (1977).
[4] For reviews see: (a) G. Ehrlich, Crit. Rev. Solid State Sci. 4, 205 (1974); (b) D. W. Bassett, in *Surface and Defect Properties of Solids*, edited by M. W. Roberts and J. M. Thomas (Chemical Society, London, 1972), Vol. 2, p. 34; (c) W. R. Graham and G. Ehrlich, Thin Solid Films 25, 85 (1975); (d) G. E. Rhead, Surf. Sci. 47, 207 (1975); (e) E. W. Muller and T. T. Tsong, *Progress in Surface Science*, edited by S. G. Davison, Vol. 4, 1, (1973). See also Refs. 17–26 cited by U. Landman and M. F. Shlesinger in Ref. 2.
[5] U. Landman, E. W. Montroll, and M. F. Shlesinger, Phys. Rev. Lett. 38, 285 (1977).
[6] K. Stolt, W. R. Graham, and G. Ehrlich, J. Chem. Phys. 65, 3206 (1976).

[7]J. E. Lennard-Jones, Proc. Phys. Soc. London, 49 (extra part), 140 (1937).
[8]J. N. Mundy, Phys. Rev. B 3, 2431 (1971).
[9]J. N. Mundy, T. E. Miller, and R. J. Porte, Phys. Rev. B 3, 2445 (1971).
[10]H. M. Gilder and D. Lazarus, Phys. Rev. B 11, 4916 (1975).
[11]R. E. Einziger and J. N. Mundy, Phys. Rev. B 17, 449 (1978).
[12]U. Landman and M. F. Shlesinger, Solid State Commun. 27, 939 (1978).
[13]N. F. Mott and R. W. Gurney, *Electronic Processes in Ionic Crystals* (Dover, New York, 1964); see also Ref. 1.
[14]See article by J. M. Blakely in *Surface Physics of Materials*, edited by J. M. Blakely (Academic, New York, 1975), and references cited therein.
[15]J. H. Sinfelt, D. L. Carter, and D. J. C. Yates, J. Catal. 24, 283 (1972).
[16]U. Landman and M. F. Shlesinger, Phys. Rev. Lett. 41, 1174 (1978); U. Landman and M. F. Shlesinger, Bull. Am. Phys. Soc. 23, 362 (1978); M. F. Shlesinger and U. Landman, presented at the 38th Annual Conference on Physical Electronics, Gatlinburg, Tennessee, 1978 (unpublished).
[17]Preceding paper, this issue. Reference to equations from that paper will be made by preceding the equation by I, e.g., (I2.34).
[18]A preliminary report of the method was given by U. Landman and M. F. Shlesinger in *Proceedings of the Thirteenth IUPAP Conference on Statistical Physics, 1977*, Ann. Isr. Phys. Soc., edited by D. Cabib, C. Kuper, and J. Reiss, Vol. 2, p. 682 (1978).
[19]M. Sugi and S. Iizima, Phys. Rev. B 15, 574 (1977).
[20]Significant effects have been observed in studies of surface diffusion in the presence of periodic arrangement of adsorbed overlayers; for reviews see H. P. Bonzel, in *Structure and Properties of Metal Surfaces*, edited by S. Shimodoira (Maruzen, Tokyo, 1973), Vol. 1; H. P. Bonzel in *Surface Physics of Materials*, edited by J. M. Blakely (Academic, New York, 1975).
[21]K. Lakatos-Lindenberg, R. P. Heminger, and R. M. Pearlstein, J. Chem. Phys. 56, 4852 (1972).
[22]R. J. Elliott, J. A. Krumhansl, and P. L. Leath, Rev. Mod. Phys. 46, 465 (1974).
[23]G. Ehrlich, in *Interatomic Potentials and Simulation of Lattice Defects*, edited by P. C. Gehlen, J. R. Beeler, Jr., and R. J. Jaffee (Plenum, New York, 1972), pp. 573–619.
[24]In a recent study, the motion of tungsten adatoms on the (100) plane of a W–3%-Re alloy was investigated by P. L. Cowan and T. T. Tsong, Surf. Sci. 67, 158 (1977).
[25]G. Ehrlich and F. G. Hudda, J. Chem. Phys. 44, 1039 (1966).
[26]A. Da. Fano and G. Jacucci, Phys. Rev. Lett. 39, 950 (1977).
[27]P. G. Shewman, *Diffusion in Solids* (McGraw-Hill, New York, 1963) p. 142.
[28]E. W. Montroll, J. Chem. Phys. 18, 734 (1950).
[29] C. M. Tchen, J. Chem. Phys. 20, 214 (1952).
[30]R. J. Rubin, J. Chem. Phys. 20, 1940 (1952).
[31]J. Gillis, Proc. Cambridge Philos. Soc. 51, 634 (1955).
[32]H. N. V. Temperley, Phys. Rev. 103, 1 (1956).
[33]C. Domb and M. E. Fisher, Proc. Cambridge Philos. Soc. 54, 48 (1958).
[34]T. Springer, *Quasielastic Neutron Scattering*, (Springer, Berlin, 1972).
[35]J. Volkl and G. Alefeld, in *Diffusion in Solids*, edited by A. S. Nowick and J. J. Burton (Academic, New York, 1975), Chap. 5.
[36]R. C. Knauer, Phys. Rev. B 3, 567 (1971).
[37]L. Van Hove, Phys. Rev. 95, 249 (1954).
[38]P. Schofield, Phys. Rev. Lett. 4, 239 (1960).
[39]C. T. Chudley and R. J. Elliott, Proc. Phys. Soc. London 77, 353 (1961).
[40](a) J. M. Rowe, in *Proceedings of the Conference on Neutron Scattering, Gatlinberg, Tennessee, 1976*, edited by R. M. Moon (National Technical Information Service, U. S. Dept. of Commerce, Springfield, Va., 1976), Vol. 1, pp. 491–506 (and references therein). (b) D. Richter, K. W. Kehr, and T. Springer in *Proceedings of the Conference on Neutron Scattering, Gatlinberg, Tennessee, 1976*, edited by R. M. Moon (National Technical Information Service, U. S. Dept. of Commerce, Springfield, Va., 1976), Vol. 1, pp. 568–574. In this paper the authors suggest the use of a two-state model for the analysis of QNS data for hydrogen diffusion in $NbH_{0.0004}N_{0.007}$ where the interstitial nitrogens acts as traps for hydrogen.
[41]K. W. Kehr and D. Richter, Solid State Commun. 20, 477 (1976); K. Schroeder, Z. Phys. B 25, 91 (1976).
[42]J. Haus and K. Kehr (unpublished).
[43]A. C. Damask and G. L. Dienes, *Point Defects in Metals* (Gordon and Breach, New York, 1971).
[44]M S. Matheson and L. M. Dorfman, *Pulse Radiolysis* (MIT, Cambridge, Mass., 1969).
[45]J. R. Clay and M. F. Shlesinger, Proc. Nat. Acad. Sci. 74, 5543 (1977).
[46]H. K. Birnbaum *et al.*, Phys. Rev. B 17, 4143 (1978).
[47]M. Borghini *et al.*, Phys. Rev. Lett. 40, 1723 (1978).
[48]S. Arnold *et al.*, J. Chem. Phys. 64, 5104 (1976).